ARTICLE IN PRESS

Available online at www.sciencedirect.com

ScienceDirect

Measurement xxx (2008) xxx–xxx

Measurement

www.elsevier.com/locate/measurement

Centralized and decentralized process and sensor fault monitoring using data fusion based on adaptive extended Kalman filter algorithm

Mohsen Mosallaei [a,*], Karim Salahshoor [a], Mohammadreza Bayat [b]

[a] *Department of Automation and Instrumentation, Petroleum University of Technology, Tehran, Iran*
[b] *Institute for Systems and Robotics (ISR), Instituto Superior Técnico (IST), Universidade Técnica de Lisboa (UTL), Lisbon, Portugal*

Received 18 October 2007; received in revised form 23 January 2008; accepted 25 February 2008

Abstract

This paper presents an integrated design framework to utilize multi-sensor data fusion (MSDF) techniques for process monitoring enhancement to detect and diagnose sensor and process faults. Two different distributed and centralized architectures are presented to integrate the multi-sensor data based on extended Kalman filter (EKF) data fusion algorithm. The distributed integration architecture uses the state-vector fusion method, while the centralized integration architecture is based on the output augmented fusion (OAF) method. The usual approach in the classical EKF implementation is based on the assumption of constant diagonal matrices for both the process and measurement covariances. This inflexible constant covariance set-up may cause degradation in the EKF performance. A new adaptive modified EKF (AMEKF) algorithm has been developed to prevent the filter divergence and hence leading to an improved EKF estimation. A set of simulation studies have been conducted to demonstrate the performances of the proposed adaptive and non-adaptive process monitoring approaches on a continuous stirred tank reactor (CSTR) benchmark problem. The sensor fault studies include the sensor faults due to drift in calibration and drift in sensor degradation anomalies. Whereas, the process faults consist of four probable CSTR faults in cascaded single, double, triple and quadruple set-up.

Keywords: Multi-sensor data fusion; Adaptive modified extended Kalman filter; Output augmented fusion; Continuous stirred tank reactor

1. Introduction

In modern chemical process industries, there has been an ever-increasing push to optimize their production processes by satisfying the continuously tightening safety and environmental regulations. Industrial processes have become more highly integrated and complex and hence their proper monitoring presents challenges that are not readily addressed using the conventional diagnosis by the operators. To ensure that the process operations are able to satisfy the increasingly stringent performance specifications, an accurate automated process monitoring is essential.

* Corresponding author. Tel.: +98 913 355 6310.
E-mail address: mohsenmosallaei@gmail.com (M. Mosallaei).

0263-2241/$ - see front matter © 2008 Elsevier Ltd. All rights reserved.
doi:10.1016/j.measurement.2008.02.009

The main goal of this automated process monitoring is to ensure the success of plant operations by recognizing anomalies of the behavior in real-time. It includes the tasks of fault detection to determine the existence of faults due to sensor or process upsets and their fault diagnosis to find the root factors causing such events.

This information keeps the plant operator and maintenance personnel better informed of the status of the process operation in order to make appropriate remedial actions to improve the abnormal behavior. As a result of this proper process monitoring, downtime is minimized, safety of plant operation is improved and manufacturing costs are reduced.

The automated fault detection and diagnosis has been an active area of research for many decades and broad spectrums of methods have been developed. Generally, depending on the rigorousness of the process knowledge employed, the existing methods can be broadly classified into two main categories of process history-based and process model-based methods. Each of these categories can further be divided into qualitative and quantitative approaches. The qualitative approaches involve fault trees [1], signed directed graph [2,3], fuzzy logic [4] and expert systems [5]. In many cases, however, these qualitative approaches simply give multiple interpretations for a single event which is an inherent limitation of the qualitative model-based methods [6]. The quantitative model-based approaches, on the other hand, utilize the process model and on-line measurements to back-calculate crucial process variables. These approaches include basically modeling, filtering and estimation techniques, where a widevariety of them have already been reviewed by [7–9]. Among the existing quantitative model-based methods, the Kalman filter variants have found widespread applications due to their simplicity and ability to handle reasonable uncertainties and nonlinearities.

The purpose of this work is to present a new automated fault detection and diagnosis system based on an enhanced extended Kalman filter (EKF) estimator. The proposed methodology utilizes a multi-sensor data fusion (MSDF) technique to enhance the accuracy and reliability of state estimation in the process fault detection. The field of multi-sensor data fusion is fairly young and most of its literature has dealt with military and civilian target tracking and autonomous robotics. This technique seeks to combine data from multiple sensors and related information to achieve improved accuracies and more specific inferences. Thus, the main problem in this paper is focused on the methodology by which the multi-sensor measurements can be combined and processed. There are various multi-sensor data fusion approaches to resolve this problem. In this work, two different multi-sensor integration architectures have been presented based on the EKF data fusion algorithm. Using the EKF, two key architecture scenarios called as centralized and decentralized or distributed methods have been developed. In the centralized integration method, called as measurement fusion integration method, all the raw data from different sensors is sent to a single location to be fused. While, in the distributed integration method, called as state-vector fusion integration method, the filtering process is divided between some local EKF filters working in parallel to obtain individual sensor-based estimates and one master EKF filter to combine these local estimates to yield an improved global state estimate. However, the operation of the EKF algorithm as the data fusion technique is critically influenced by uncertainty in covariance parameters of the process noise (Q) and the observation error (R).

In this paper, an online adaptive scheme has been developed to enhance the EKF estimation procedure based on the innovation and residual sequences of the EKF algorithm. As a consequence, three different process monitoring approaches, called as non-adaptive centralized output augmented fusion (NACOAF), adaptive centralized output augmented fusion (ACOAF) and adaptive distributed state-vector fusion (ADSVF) have been proposed in this paper.

The paper is organized as follows. The model-based process fault monitoring problem is formulated in Section 2. In Section 3, first, a discrete-time EKF algorithm is presented. Then, an adaptive EKF is developed. Finally, two different centralized and distributed multi-sensor integration architectures combined with the adaptive EKF data fusion will be presented. Simulation studies illustrating the performances of the three proposed process monitoring approaches (i.e., NACOAF, ACOAF and ADSVF) are evaluated for sensor and process fault detection and diagnosis in Section 4. In Section 5, the main concluding remarks are summarized.

2. Formulation of model-based process fault monitoring problem

Instrumentation sensors are usually distributed throughout the chemical process plants to meet

Please cite this article in press as: M. Mosallaei et al., Centralized and decentralized process and sensor ..., Measurement (2008), doi:10.1016/j.measurement.2008.02.009

both operational and safety requirements. However, this scheme introduces a number of complications which makes the consolidation of the data from the located sensors a complicated task even for an experienced engineer. Further complications include the nature of information obtained from the sensors which is inherently incomplete, uncertain, and imprecise. Hence, it is imperative that a fusion mechanism be devised so as to combine data from multiple sensors to minimize such imprecision and uncertainty, leading to a more comprehensive and unified view of the sensor data.

These conditions combined with the requirements for a model-based approach to provide any process failure detection and diagnosis information make the Kalman filter (KF) approach an ideal solution for the data fusion problem. However, the effectiveness of such approach depends to a large extent on how redundant and complementary are the information cues obtained from the installed sensors and the KF estimation. It is equally important to decide at what level of abstraction the fusion process is going to take place, e.g., at the measurement level, at the feature/state level, or at the decision level.

The main issue in this model-based approach concerns the ability to detect and diagnose the process faults using the dependencies between the different process observed or estimated variables. These dependencies can be explored by considering mathematical process and measurement models.

Assume that the process is monitored by N different sensors, described by the following general nonlinear process and measurement models in discrete-time state-space framework:

$$x(k) = f(x(k-1), u(k-1), d(k-1)) + w(k-1) \tag{1}$$

$$z_i(k) = h_i(x(k)) + v_i(k); \quad i = 1, \ldots, N \tag{2}$$

where $f(\cdot)$ and $h_i(\cdot)$ are the known nonlinear functions, representing the state transition model and the measurement model, respectively. $x(k) \in R^{n_x}$ is the process state-vector, $u(k) \in R^{n_u}$ denotes the manipulated process variables, $d(k) \in R^{n_d}$ represents the process faults modeled by the process disturbances, $z_i(k) \in R^{n_{zi}}$ are the measured variables obtained from the N installed sensors, $w(k)$ and $v_i(k)$ indicate the stochastic process and measurement disturbances modeled by zero-mean white Gaussian noises with covariance matrices $Q(k)$ and $R_i(k)$, respectively.

Therefore, the process fault monitoring problem in this paper can be reduced to a design methodology to realize a data integration mechanism which is able to fuse together the N noisy measured data $(z_i(k);\ i = 1, \ldots, N)$, given in Eq. (2), to generate the optimal detection and diagnostic estimation information $(\hat{x}(k))$ about the real-time status of the nonlinear process operation, described by Eq. (1).

The central challenges of this design problem, however, can specifically be expressed in terms of the data fusion algorithm by which the multi-sensor measured data are fused together and the data integration architecture approach to determine the fusion level and its implementation topology.

3. Multi-sensor data fusion technique based on extended Kalman filter algorithm

Multi-sensor data fusion(MSDF) is a synergistic process, concerning the mechanism of fusing uncertain, incomplete, and sometimes conflicting data from a variety of disparate sensors in real time to extract a single compilation of the overall system status for monitoring, control and decision-making purposes.

For a particular industrial process application, there might be plenty of associated sensor measurements located at different operational levels and having various accuracy and reliability specifications. One of the key issues in developing a MSDF system is the question of how can the multi-sensor measurements be fused or combined to overcome uncertainty associated with individual data sources and obtain an accurate joint estimate of the system state vector. There exists various approaches to resolve this MSDF problem, of which the KF is one of the most significant and applicable candidate solution.

3.1. Discrete-time extended Kalman filter

In most practical applications of interest, the process and/or measurement dynamic models are described by nonlinear equations, represented in Eqs. (1) and (2). This means that the non-linear behavior can affect the process operation at least through its own process dynamics or measurement equation. In such cases, the standard KF algorithm is often unsuitable to estimate the process states using its linearized time-invariant state-space model at the desired process nominal operating point.

Please cite this article in press as: M. Mosallaei et al., Centralized and decentralized process and sensor ..., Measurement (2008), doi:10.1016/j.measurement.2008.02.009

Extended Kalman filter (EKF) gives a simple and effective remedy to overcome such nonlinear estimation problem. Its basic idea is to locally linearize the nonlinear functions, described by Eqs. (1) and (2), at each sampling time instant around the most recent process condition estimate. This allows the Kalman filter to be applied to the following linearized time-varying model:

$$x(k) = A(k)x(k-1) + B_u(k)u(k-1) + B_d(k)d(k-1) + w(k-1) \quad (3)$$

$$z_i(k) = H_i(k)x(k) + v_i(k); \quad i = 1, \ldots, N \quad (4)$$

where the state transition matrix $A(k)$, the input matrices $B_u(k)$ and $B_d(k)$, and the observation matrix $H_i(k)$ are the Jacobian matrices which are evaluated at the most recent process operating condition in real-time rather than the process fixed nominal values:

$$A(k) = \left.\frac{\partial f}{\partial x}\right|_{\hat{x}(k)} \quad (5)$$

$$B_u(k) = \left.\frac{\partial f}{\partial u}\right|_{u(k)} \quad (6)$$

$$B_d(k) = \left.\frac{\partial f}{\partial d}\right|_{\hat{d}(k)} \quad (7)$$

$$H_i(k) = \left.\frac{\partial h_i}{\partial x}\right|_{\hat{x}(k)}, \quad i = 1, \ldots, N \quad (8)$$

In classical control, disturbance variables $d(k)$ are treated as known inputs with distinct entry in the process state-space model. This distinction between state and disturbance as non-manipulated variables, however, is not justified from the monitoring perspective using the EKF estimation procedure. Therefore, a new augmented state variable vector $x^*(k) = [d^{\mathrm{T}}(k)x^{\mathrm{T}}(k)]^{\mathrm{T}}$ is developed by considering the process disturbances or faults as additional state variables. To implement this view, the process faults are assumed to be random state variables governed by the following stochastic auto-regressive (AR) model equation:

$$d(k) = d(k-1) + w_d(k-1) \quad (9)$$

This assumption changes the linearized model formulations in Eqs. (3) and (4) to the following augmented state-space model:

$$x^*(k) = A^*(k)x^*(k-1) + B^*(k)u(k-1) + w^*(k-1) \quad (10)$$

$$z_i(k) = H_i^*(k)x^*(k) + v_i(k), \quad i = 1, \ldots, N \quad (11)$$

Noting that:

$$A^*(k) = \begin{bmatrix} I^{n_d \times n_d} & 0^{n_d \times n_x} \\ B_d(k)^{n_x \times n_d} & A(k)^{n_x \times n_x} \end{bmatrix} \quad (12)$$

$$B^*(k) = \begin{bmatrix} 0^{n_d \times n_u} & B_u(k)^{n_x \times n_u} \end{bmatrix}^{\mathrm{T}} \quad (13)$$

$$H_i^*(k) = \begin{bmatrix} 0^{1 \times n_d} & H_i(k)^{1 \times n_x} \end{bmatrix} \quad (14)$$

$$w^*(k-1) = \begin{bmatrix} w_d(k-1)^{n_d \times 1} & w(k-1)^{n_x \times 1} \end{bmatrix}^{\mathrm{T}} \quad (15)$$

where n_x and n_u denote the dimensions of the state vector (x) and the manipulated variables (u), respectively, and n_d indicates the dimension of the disturbance or non-manipulated variables (d).

In practice, the process dynamic model in Eq. (1) is of continuous-time nature. While, the measurements in Eq. (2) are available through the digital data-acquisition systems at discrete time instants. Furthermore, the EKF algorithm is implemented digitally to provide a quick and accurate estimate of the process variables of interest. Therefore, an efficient formulation of the algorithm needs to be made for a real-time practical implementation in order to minimize the filter cycle time, while obtaining a reasonable state estimate accuracy. An appropriate method can be used for numerical integration of the continuous-time process model from one sample time to the next. In this paper, the simple first-order Euler integration algorithm has shown to be adequate. The time propagation equation for the state covariance matrix $P(k)$ is solved using the transition matrix technique [10]. This method preserves both the symmetry and the positive definiteness of $P(k)$, and hence yields adequate estimation performance:

$$P^-(k) = \Phi(k)P(k-1)\Phi^{\mathrm{T}}(k) + Q_d(k) \quad (16)$$

where $\Phi(k)$ denotes the state transition matrix associated with $A(k)$ for all the time interval $\tau \in [(k-1)T_s, kT_s]$ which can be evaluated by:

$$\Phi(k) = I + T_s A^*(k) \quad (17)$$

where T_s is the sampling period and $Q_d(k)$ is calculated as follows:

$$Q_d(k) = \int_{(k-1)T_s}^{kT_s} \Phi(kT_s, \tau)Q(\tau)\Phi^{\mathrm{T}}(kT_s, \tau)\mathrm{d}\tau \quad (18)$$

As a result, $Q_d(k)$ can be obtained using the following trapezoidal integration scheme:

$$Q_d(k) = (\Phi(k)Q(k)\Phi^{\mathrm{T}}(k) + Q(k))\frac{T_s}{2} \quad (19)$$

The EKF is then implemented using the time update equations which project the state and covariance

estimates forward one time step, and the measurement update equations which correct the state and covariance estimates using the latest measurement information, are summarized as follows:

EKF time update equations

(1) $\hat{x}^{*-}(k) = \hat{x}^{*}(k-1) + T_s f(\hat{x}^{*}(k-1), u(k-1), \hat{d}(k-1))$
(2) $P^{-}(k) = \Phi(k)P(k-1)\Phi^{\mathrm{T}}(k) + Q_d(k)$

EKF measurement update equations

(1) $K(k) = P^{-}(k)H_i^{*\mathrm{T}}(k)[H_i^{*}(k)P^{-}(k)H_i^{*\mathrm{T}}(k) + R(k)]^{-1}$
(2) $\hat{x}^{*}(k) = \hat{x}^{*}(k-1) + K(k)[z_i(k) - H_i^{*}(k)\hat{x}^{*-}(k)]$
(3) $P(k) = P^{-}(k) - K(k)H_i^{*}(k)P^{-}(k)$

The covariance matrix can be initialized ($P(0)$) with a large value. This option, however, causes rapid fluctuations in the initial EKF state estimates and hence endangers the estimator convergence. On the other hand, choosing a small initial covariance matrix will make the estimator adaptation very slow. Furthermore, when the process dynamics change, the old estimated information will lose its significance as far as the new process dynamic is concerned. Thus, there should be a means of draining off old information at a controlled rate. One simple and useful way of rationalizing this desired approach is to modify the covariance matrix update relationship as follows:

$$P(k) = [P^{-}(k) - K(k)H_i^{*}(k)P^{-}(k)]/\lambda \tag{20}$$

where $0 < \lambda \leqslant 1$ behaves as the forgetting factor concept in the weighted recursive least squares (WRLS) algorithm.

3.1.1. Adaptive extended Kalman filter (AEKF)

The operation of the EKF algorithm as the data fusion technique relies on the precise a priori knowledge of the process and measurement dynamic models and their noise properties. The uncertainty in the covariance parameters of the process noise (Q) and the observation error (R) has a crucial impact on the EKF performance and may significantly degrade its performance. This is due to the fact that Q and R influence the weight that the EKF applies between the existing process information and the latest measurements. Hence, errors in any of them may cause the EKF to diverge.

The conventional way of determining Q and R requires good a priori knowledge of the process noise and measurement error, which typically comes from intensive empirical analysis. In practice, however, their values are generally assumed to be fixed during the whole process of estimation time interval. The resulting EKF performance suffers due to this inflexibility scheme, because, process and measurement noises are dependent on the application environment and process dynamics. Thus, their settings in different applications have to be done conservative in order to stabilize the EKF for the worst case scenario, leading to performance degradation.

In this paper, an online scheme is presented to prevent the EKF degradation and divergence. It is well known that the innovation and residual sequences of the EKF are reliable indicators of its filtering performance. The innovation sequence is defined as

$$\eta_i(k) = z_i(k) - H_i^{*}(k)\hat{x}^{*-}(k) \tag{21}$$

and the residual sequence as

$$\varepsilon_i(k) = z_i(k) - H_i^{*}(k)\hat{x}^{*}(k) \tag{22}$$

Substituting the measurement model (Eq. (11)) into Eq. (21), gives:

$$\begin{aligned}\eta_i(k) &= (H_i^{*}(k)x^{*}(k) + v_i(k)) - H_i^{*}(k)\hat{x}^{*-}(k) \\ &= H_i^{*}(k)[x^{*}(k) - \hat{x}^{*-}(k)] + v_i(k)\end{aligned} \tag{23}$$

On the other hand, we have:

$$e_k^{*-} \cong x^{*}(k) - \hat{x}^{*-}(k) \tag{24}$$

$$e_k^{*} \cong x^{*}(k) - \hat{x}^{*}(k) \tag{25}$$

$$P^{-}(k) = E[e_k^{*-}e_k^{*-\mathrm{T}}] \tag{26}$$

$$P(k) = E[e_k^{*}e_k^{*\mathrm{T}}] \tag{27}$$

$$R_i = E[v_i(k)v_i(k)^{\mathrm{T}}] \tag{28}$$

For an optimal EKF operation, the innovation and residual sequences should be white Gaussian noise sequences with zero mean. On the basis of assuming that $w^{*}(k)$ and $v_i(k)$ are uncorrelated white Gaussian noise sequences and the orthogonality condition exists between observation error and state estimation error, the innovation covariance can be computed from Eq. (23):

$$\begin{aligned}E[\eta_i(k)\eta_i^{\mathrm{T}}(k)] &= E[(H_i^{*}(k)e_k^{*-})(H_i^{*}(k)e_k^{*-})^{\mathrm{T}}] \\ &\quad + E[v_i(k)v_i^{\mathrm{T}}(k)] \\ &= H_i^{*}(k)E[e_k^{*-}e_k^{*-T}]H_i^{*\mathrm{T}}(k) + R_i(k)\end{aligned} \tag{29}$$

That is

$$R_i(k) = E[\eta_i(k)\eta_i^{\mathrm{T}}(k)] - H_i^*(k)P^-(k)H_i^{*\mathrm{T}}(k), \quad i = 1, \ldots, N \tag{30}$$

Thus, when the innovation covariance $E[\eta_i(k)\eta_i^{\mathrm{T}}(k)]$ is available, the covariance of the observation error $R_i(k)$ can be estimated directly from Eq. (30). Calculation of the residual covariance$E[\eta_i(k)\eta_i^{\mathrm{T}}(k)]$ normally uses a limited number of samples of the innovation sequence:

$$E[\eta_i(k)\eta_i^{\mathrm{T}}(k)] = \frac{1}{M}\sum_{m=0}^{M-1}\eta_i(k-m)\eta_i^{\mathrm{T}}(k-m) \tag{31}$$

in which M represents the estimation window size. However, it is noted that Eq. (31) gives a valid result when the innovation sequence is stationary and ergodic over the M sample steps.

To improve the robustness of the adaptive filtering algorithm to innovation and residual covariance estimations, a new process noise method is proposed here as follows:

$$\eta_i(k) - \varepsilon_i(k) = H_i^*(k)[\hat{x}^*(k) - \hat{x}^{*-}(k)] \tag{32}$$

Noting that the process output variables in our formulation are always the same as the process state variables, implying that $H_i^*(k) = I$. Hence, Eq. (32) will be reduced to $\eta_i(k) - \varepsilon_i(k) = \hat{x}^*(k) - \hat{x}^{*-}(k)$. Thus, it can be written:

$$(\eta_i(k) - \varepsilon_i(k))^{\mathrm{T}} = [\hat{x}^*(k) - \hat{x}^{*-}(k)]^{\mathrm{T}} \tag{33}$$

Multiplying Eq. (32) into Eq. (33) and taking the expectation operator from its both sides, gives:

$$(\eta_i(k) - \varepsilon_i(k))(\eta_i(k) - \varepsilon_i(k))^{\mathrm{T}} = [\hat{x}^*(k) - \hat{x}^{*-}(k)][\hat{x}^*(k) - \hat{x}^{*-}(k)]^{\mathrm{T}} \tag{34}$$

$$E[\eta_i(k)\eta_i^{\mathrm{T}}(k)] + E[\varepsilon_i(k)\varepsilon_i^{\mathrm{T}}(k)] = E[(\hat{x}^*(k) - \hat{x}^{*-}(k))(\hat{x}^*(k) - \hat{x}^{*-}(k))^{\mathrm{T}}] = E[(e_k^{*-} - e_k^*)(e_k^{*-} - e_k^*)^{\mathrm{T}}] = P^-(k) + P(k) \tag{35}$$

On the other hand, the residual covariance can be approximated as follows:

$$E[\varepsilon_i(k)\varepsilon_i^{\mathrm{T}}(k)] = \frac{1}{M}\sum_{m=0}^{M-1}\varepsilon_i(k-m)\varepsilon_i^{\mathrm{T}}(k-m) \tag{36}$$

When the residual covariance $E[\varepsilon_i(k)\varepsilon_i^{\mathrm{T}}(k)]$is available, the covariance of the process error $Q_d(k)$ can be estimated from substituting equations (16), (31), (36) into Eq. (35):

$$Q_d(k) = [\frac{1}{M}\sum_{m=0}^{M-1}(\eta_i(k-m)\eta_i^{\mathrm{T}}(k-m) + \varepsilon_i(k-m)\varepsilon_i^{\mathrm{T}}(k-m))] - [\Phi(k)P(k-1)\Phi^{\mathrm{T}}(k) + P(k)] \tag{37}$$

3.2. Multi-sensor integration architectures based on Kalman filter data fusion algorithm

Multi-sensor data fusion can be done at a variety of levels from the raw data or observation level to the feature/state vector level and the decision level. This idea can lead to utilization of different possible configurations or architectures to integrate the data from disparate sensors in an industrial plant to extract the desired monitoring information. Using Kalman filtering as the data fusion algorithm, multiple sensors can be integrated in two key architecture scenarios called centralized method and decentralized or distributed method. These methods have been widely studied over the last decade [11,12]. In centralized integration method, all the raw data from different sensors is sent to single location to be fused, as shown in Fig. 1.

This architecture is sometimes called as measurement fusion integration method [11,12], in which observations or sensor measurements are directly fuses to obtain a global or combined measurement data matrix (H^*). Then, it uses a single Kalman filter to estimate the global state vector based upon the fused measurement. Although this conventional method provides high fusion accuracy to the estimation problem, the large number of states may require high processing data rates that cannot be maintained in practical real time applications. Another disadvantage of this method is the lack of robustness in case of failure in sensor or central filter itself. For these reasons, parallel structures can often provide improved failure detection and correction, enhance redundancy management, and decreased costs for multi-sensor system integration. As such, there has recently been considerable interest shown in distributed integration method in which the filtering process is divided between some local Kalman filters working in parallel to obtain individual sensor-based state estimates and one master filter combining these local estimates to yield an improved global state estimate, as shown in Fig. 2. This architecture is sometimes called as state-vector fusion integration method [11,12]. The advantages of this method are higher robustness

Please cite this article in press as: M. Mosallaei et al., Centralized and decentralized process and sensor ..., Measurement (2008), doi:10.1016/j.measurement.2008.02.009

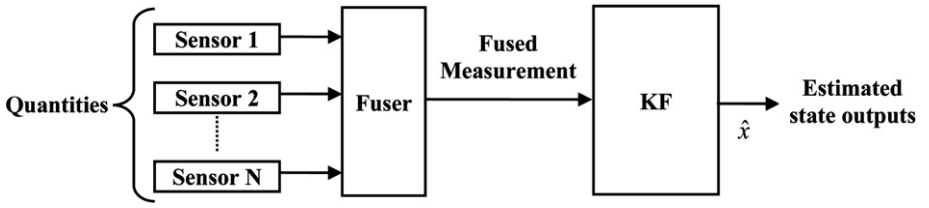

Fig. 1. Centralized integration architecture.

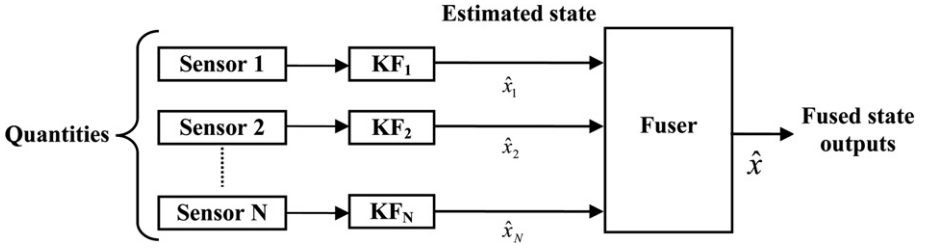

Fig. 2. Distributed integration architecture.

due to parallel implementation of fusion nodes and lower computation load and communication cost at each fusion node. It is also applicable in modular systems where different process sensors can be provided as separate units. On the other hand, distributed fusion is conceptually a lot more complex and is likely to require higher bandwidth compared with centralized fusion. However, a trade-off between bandwidth and performance is possible by letting the fusion nodes communicate at reduced rates [13].

3.2.1. Centralized integration method based on EKF data fusion algorithm

In the presented centralized integration method, the data from all the local sensors is fed into a data fusion center where all the process measurements are processed centrally by the EKF data fusion algorithm to yield the global process state estimate.

Assume that the nonlinear dynamic process to be monitored is described by the augmented state-space model, given in Eq. (10). Accordingly, the process measurement system, including N different sensors, has the following dynamic model (Eq. (11)):

$$z_i(k) = H_i^*(k)x^*(k) + v_i(k), \quad i = 1, \ldots, N \tag{38}$$

where $z_i(k)$ represents the ith sensor measurement data and $H_i^*(k)$ indicates its corresponding linearized measurement matrix.

The centralized fusion problem is concerned with different formulation methods by which the observation data (z_i, $i = 1,\ldots, N$) can be combined to transform the N measurement equations described by Eq. (38) into the following single measurement equation:

$$z(k) = H^*(k)x^*(k) + v(k) \tag{39}$$

where $H^*(k)$ indicates a single observation matrix, called as global observation matrix and $v(k)$ denotes the overall measurement noise vector $[v_1(k)\ v_2(k) \ldots v_N(k)]^{\mathrm{T}}$ based on the assumption that $v_i(k)$ are independent.

3.2.1.1. Centralized integration method using outputs augmented fusion (OAF) formulation. The observation data (z_i) can simply be combined by augmenting the multi-sensor data, leading to the following observation model:

$$z(k) = [z_1^{\mathrm{T}}(k) \ldots z_N^{\mathrm{T}}(k)]^{\mathrm{T}} \tag{40}$$

$$H^*(k) = [H_1^{*\mathrm{T}}(k) \ldots H_N^{*\mathrm{T}}(k)]^{\mathrm{T}} \tag{41}$$

$$R(k) = \mathrm{diag}[R_1(k) \ldots R_N(k)] \tag{42}$$

It is then straightforward to apply the discrete-time EKF algorithm as the global data fusion algorithm in centralized integration architecture to obtain fused measurement information.

This method makes use of all the raw measurement information in their original form without any dimension reduction in the observation model.

Please cite this article in press as: M. Mosallaei et al., Centralized and decentralized process and sensor ..., Measurement (2008), doi:10.1016/j.measurement.2008.02.009

Thus, it is applicable in all situations such as dissimilar sensors whose measurement matrices might be of different sizes. However, its computational load increases with adding more sensors.

3.2.2. Distributed state-vector integration method based on the modified track-to-track fusion (MTTF) algorithm

The standard track-to-track fusion (TTF) algorithm is an alternative approach to optimally combine the local state estimations. In this approach, the individual and local estimations (i.e., $\hat{x}_i(k|k)$) are fed back to the predictive stage of the Kalman filtering process corresponding to each individual sensor. This makes the state estimations $\hat{x}_i(k|k)$ be mutually dependent. A better approach has been introduced by the MTTF algorithm in which the prediction procedure of the Kalman filtering will be improved by the fused state estimation $\widehat{X}(k|k-1)$ at the last time step instead of the individual or local state estimation (i.e., $\hat{x}_i(k|k)$) in the standard TTF algorithm. In this paper, the MTTF algorithm, shown in Fig. 3, has been employed for the proposed distributed integration method. The new fused estimation $\widehat{X}(k|k)$ and the covariance matrix of the fused estimation are derived by the following equations:

$$\widehat{X}(k|k) = \hat{x}_1(k|k) + \frac{1}{N-1}\sum_{i=2}^{N}[P_1(k|k) - P_{1i}(k|k)] \times [P_1(k|k) + P_i(k|k) - P_{1i}(k|k) - P_{i1}(k|k)]^{-1} \times [\hat{x}_i(k|k) - \hat{x}_1(k|k)] \quad (43)$$

$$P(k|k) = P_1(k|k) - \frac{1}{N-1}\sum_{i=2}^{N}[P_1(k|k) - P_{1i}(k|k)] \times [P_1(k|k) + P_i(k|k) - P_{1i}(k|k) - P_{i1}(k|k)]^{-1} \times [P_1(k|k) - P_{i1}(k|k)] \quad (44)$$

4. Simulation studies

A major objective of this research is to investigate the usefulness of different multi-sensor integration architectures based on the EKF data fusion algorithm to detect and diagnose sensor and process faults. The basic idea of the adapted monitoring approach is to reconstruct the process states from the available multi-sensor data measurements integrated in two centralized and decentralized configurations using the EKF algorithm for both state estimation and data fusion purposes. Two general types of sensor and process faults are realized in a simulation continuous stirred tank reactor (CSTR) as a typical chemical benchmark problem.

4.1. CSTR plant description

The CSTR represented schematically in Fig. 4 works under atmospheric pressure [14]. It is a cooling water-jacketed reactor which involves an irreversible and liquid phase exothermic reaction $A \rightarrow B$ taking place inside the reactor tank. The cooling jacket surrounding the reactor circulates the coolant water to absorb the generated reaction heat.

Two proportional controllers are used to regulate the reactor outlet temperature (T) and the liquid volume (V) inside the reactor tank. The temperature is controlled by manipulating the flow rate of the coolant water ($u_1 = F_j$) following through the jacket. While, the level in the reactor is controlled by manipulating the outlet flow rate ($u_2 = F_o$) from the reactor.

The dynamic behavior of the CSTR is modeled by a system of differential equations translating molar and heat balances in the reactor. The derived model is based on the following hypotheses:

- The reactor is perfectly stirred implying that the reaction mass temperature and concentrations are homogeneous through the mass volume.

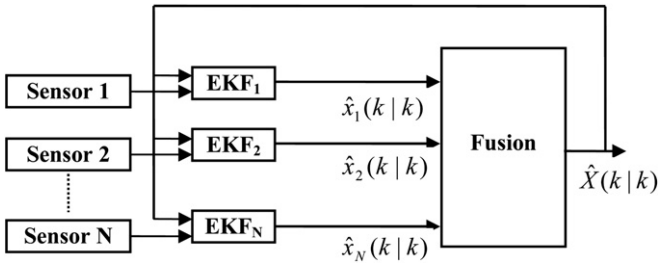

Fig. 3. The modified (T–T) fusion algorithm.

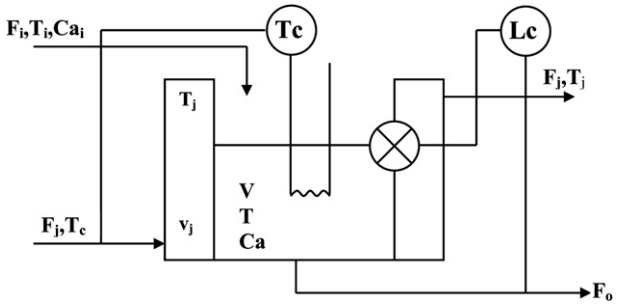

Fig. 4. Continuous stirred tank reactor.

- The heat losses are negligible.
- No phase change occurs in the reaction mass.
- The density, the specific heat of the cooling and the reaction mass heat are independent of the temperature.
- Constant holdup and perfect mixing are assumed in the cooling jacket.

The resulting CSTR plant model equations can be described by [14]:

$$\frac{dV}{dt} = F_i - F_o \tag{45}$$

$$\frac{d(VCa)}{dt} = F_i Ca_i - F_o Ca - V\left(k_0 \exp\left(\frac{E_a}{RT}\right)\right)Ca \tag{46}$$

$$\rho c_p \frac{d(VT)}{dt} = \rho c_p (F_i T_i - F_o T) - \Delta H V \times \left(k_o \exp\left(\frac{E_a}{RT}\right)\right)Ca - Ua_0(T - T_j) \tag{47}$$

$$\rho_j V_j c_j \frac{dT_j}{dt} = \rho_j c_j F_j (T_c - T_j) + Ua_0(T - T_j) \tag{48}$$

$$F_o = 40 - 10(48 - V)$$
(Proportional level controller) (49)

$$F_j = 49.9 - 4(600 - T)$$
(Proportional temperature controller) (50)

The derived model equations are modified to be formulated in terms of the normalized and dimensionless states by the main process variables (F_i, Ca_i, T_i, T_c) to be monitored. The resulting state equations include the explicit fault terms $(\Delta F_i, \Delta Ca_i, \Delta T_i, \Delta T_c)$, as follows [15]:

$$\frac{dx_1}{dt} = \frac{F_i}{V_s} - \frac{F_{os}}{V_s}(u_1 + 1) + \frac{1}{1 + \frac{Ca_i}{Ca_s} + \frac{T_i}{T_s}} \Delta F_i \left(\frac{1}{V_s} + \frac{Ca_i}{V_s Ca_s} + \frac{T_i}{V_s T_s}\right) \tag{51}$$

$$\frac{dx_2}{dt} = \frac{F_i Ca_i}{V_s Ca_s} - \frac{F_{os}(u_1 + 1)(x_2 + 1)}{V_s(x_1 + 1)} - k_0(x_2 + 1)\exp\left(\frac{-E_a(x_1 + 1)}{RT_s(x_3 + 1)}\right) + \frac{Ca_i}{Ca_s + Ca_i + \frac{Ca_s T_i}{T_s}} \Delta F_i \left(\frac{1}{V_s} + \frac{Ca_i}{V_s Ca_s} + \frac{T_i}{V_s T_s}\right) + \Delta Ca_i \frac{F_i}{V_s Ca_s} \tag{52}$$

$$\frac{dx_3}{dt} = \frac{F_i T_i}{V_s T_s} - \frac{F_{os}(u_1 + 1)(x_3 + 1)}{V_s(x_1 + 1)} - \frac{\Delta H Ca_s k_0}{\rho c_p T_s} \times (x_2 + 1)\exp\left(\frac{-E_a(x_1 + 1)}{RT_s(x_3 + 1)}\right) - \frac{Ua_0(x_3 + 1)}{\rho c_p V_s(x_1 + 1)} + \frac{Ua_0 T_{js}(x_4 + 1)}{\rho c_p V_s T_s} + \Delta T_i \frac{F_i}{V_s T_s} + \frac{T_i}{T_s + \frac{Ca_i T_s}{Ca_s} + T_i} \Delta F_i \left(\frac{1}{V_s} + \frac{Ca_i}{V_s Ca_s} + \frac{T_i}{V_s T_s}\right) \tag{53}$$

$$\frac{dx_4}{dt} = \frac{T_c F_{js}}{V_j T_{js}}(u_2 + 1) - \frac{F_{js}(u_2 + 1)(x_4 + 1)}{V_j} + \left(\frac{Ua_0 T_s (x_3 + 1)}{\rho_j c_j V_j T_{js}(x_1 + 1)} - \frac{Ua_0(x_4 + 1)}{\rho_j c_j V_j}\right) + \Delta T_c \frac{F_{js}(u_2 + 1)}{V_j T_{js}} \tag{54}$$

where

$$x_1 = \frac{V - V_s}{V_s}, \quad x_2 = \frac{VCa - V_s Ca_s}{V_s Ca_s}, \quad x_3 = \frac{VT - V_s T_s}{V_s T_s}, \quad x_4 = \frac{T_j - T_{js}}{T_{js}}, \quad u_1 = \frac{F_o - F_{os}}{F_{os}}, \quad u_2 = \frac{F_j - F_{js}}{F_{js}} \tag{55}$$

Please cite this article in press as: M. Mosallaei et al., Centralized and decentralized process and sensor ..., Measurement (2008), doi:10.1016/j.measurement.2008.02.009

The relevant parameters for simulating the CSTR plant are tabulated in Table 1. The table includes the steady-state condition of the reactor indicated by the subscript "s" as V_s, Ca_s, T_s, T_{js}, F_{os}, F_{js} at normal operating point.

4.2. Formulation of plant state equations for fault monitoring

The CSTR plant dynamic model in Eqs. (51)–(54) demonstrate its nonlinear dynamic nature which can be represented by the following general nonlinear state equations ($f_i(\cdot)$; $i = 1,\ldots,4$) in discrete-time domain:

$$x_1(k+1) = f_1(x(k), u(k), d(k)) + w_1(k-1) \quad (56)$$

$$x_2(k+1) = f_2(x(k), u(k), d(k)) + w_2(k-1) \quad (57)$$

$$x_3(k+1) = f_3(x(k), u(k), d(k)) + w_3(k-1) \quad (58)$$

$$x_4(k+1) = f_4(x(k), u(k), d(k)) + w_4(k-1) \quad (59)$$

where k denotes the sampling instants and

$$x(k) = [x_1(k) \quad x_2(k) \quad x_3(k) \quad x_4(k)]^{\mathrm{T}} \quad \text{(State vector)} \quad (60)$$

$$u(k) = [u_1(k) \quad u_2(k)]^{\mathrm{T}} \quad \text{(Input vector)} \quad (61)$$

$$d(k) = [\Delta F_i(k) \quad \Delta Ca_i(k) \quad \Delta T_i(k) \quad \Delta T_c(k)]^{\mathrm{T}} \quad \text{(Process fault vector)} \quad (62)$$

$w_i(k-1)$; $i = 1,\ldots,4$, describe the process noises which have been added artificially to the CSTR process state model equations to include the real uncertainties faced in the practical situations. These process noises are assumed to behave as zero-mean white Gaussian noises with covariance matrix $Q(k)$. Similarly, the output equation can be described by the following general nonlinear model ($h(\cdot)$), derived from the CSTR dynamic model in Eqs. (51)–(54):

$$y(k) = h(x^*(k)) + v(k) \quad (63)$$

where $x^*(k) = [d^{\mathrm{T}}(k) \quad x^{\mathrm{T}}(k)]^{\mathrm{T}}$ represents the augmented state variable vector, $v(k) = [v_1(k), v_2(k), v_3(k), v_4(k)]^{\mathrm{T}}$ has been added to represent the inevitable measurement noises and $y(k)$ denotes the output vector. $v(k)$ is assumed to behave as zero-mean white Gaussian noises with covariance matrix $R(k)$. Therefore, the nonlinear functions $f(\cdot) = [f_1(\cdot), f_2(\cdot), f_3(\cdot), f_4(\cdot)]^{\mathrm{T}}$ and $h(\cdot)$ in state and output model equations can be linearized at each sampling time around the most recent process condition estimate, leading to the augmented state-space model given by Eqs. (10) and (11).

Table 1
Non-isothermal CSTR parameters

Notation	Variable	Steady state values
F_o	Outlet flow rate	40 ft^3/h (F_{os})
Ca_i	Inlet reactant concentration	0.5 lb mol of A/ft^3 (Ca_{is})
T	Temperature of tank	600 °R (T_s)
F_j	Coolant flow rate	49.9 ft^3/h (F_{js})
V	Volume of reactor	48 ft^3 (V_s)
Ca	Outlet reactant concentration	0.245 lb mol of A/ft^3(Ca_s)
T_j	Temperature of the outlet coolant	594.6 °R (T_{js})
T_i	Inlet feed temperature	530 °R (T_{is})
		Parameter values
V_j	Volume of jacket	3.85 ft^3
E_a	Activation energy	30,000 Btu/lb mol
U	Heat-transfer coefficient	150 Btu/h ft^2 °R
T_c	Temperature of the inlet coolant	530 °R
c_p	Heat capacity (process side)	0.75 Btu/lbm °R
ρ	Density of process mixture	50 lbm/ft^3
k_0	Frequency factor	$7.08 \times 1010\ \mathrm{h}^{-1}$
R	Universal gas constant	1.99 Btu/lb mol °R
a_0	Heat-transfer area	250 ft^2
ΔH	Heat of reaction	−30,000 Btu/lb mol
C_j	Heat capacity (coolant side)	1.0 Btu/lbm °R
ρ_j	Density of coolant	62.3 lbm/ft^3

For computer simulation of the plant fault monitoring studies, the CSTR nonlinear model dynamics, described in Eqs. (56)–(59), are implemented using s-function and SIMULINK facilities in MATLAB. The basic time unit is hours (h) and the sampling time is taken to be equal to 0.005 h.

4.3. Sensor fault detection and diagnosis

A sensor often comprises of different parts such as a sensing device, transducer, signal processor, and communication interface. Any of these parts may malfunction causing the sensor to generate signals with unacceptable deviation from its normal condition. A sensor working under this condition, i.e. faulty sensor, may cause process performance degradation, process shut-down or even fatal accidents. A sensor is declared faulty when it displays a non-permitted deviation from the characteristic properties.

This study focuses on drift in sensor calibration (i.e., bias error) and drift in sensor degradation (i.e., excessive-variance noise) anomalies. A sensor

is biased if its reading differs by a constant value from the actual value. The excessive-variance noise fault refers to the case where the sensor reading is affected by an excessive-variance white noise. This fault might represent the gradual or incipient sensor degradation due to wear, aging, fouling or corrosion which is generally not detectable in their early stages.

4.3.1. Drift in sensor calibration (bias error)

To carry out the sensor calibration fault detection, a method is required to quantity the state derivation due to sensor fault occurrence. The following stochastic AR model is employed to explain the time evolution of the sensor bias as extra process state variables

$$b_i(k) = b_i(k-1) + N_{b_i}(k), \quad i = 1, \ldots, n_b \tag{64}$$

where n_b denotes the number of faulty sensors, and $N_{bi}(k)$ indicates a zero-mean white Gaussian noise with covariance matrices $Q_{bi}(k)$ describing the bias model uncertainty. Therefore, the process state variable vector in Eqs. (10) and (11) is augmented by the sensor bias states, defined in Eq. (64).

Table 2
Sensor fault scenario in the key variable sensors

Sensor fault parameter	The magnitude of fault			
	V	T	Ca	T_j
Bias	5	0.03	−30	60
Excessive-variance coefficient	0.5	0.01	2	2.5

4.3.2. Drift in sensor degradation (excessive-variance noise)

To simulate this type of sensor fault, the following model equation is used to describe an added sensor white noise whose variance characteristic is changed linearly with time evolution.

$$n(k) = \sigma_0 \frac{k-1}{T_{\max}/1.5 - 1} N_n(k) \tag{65}$$

where σ_0 shows the coefficient noise variance, $T_{\max}$ indicates the maximum number of measurement

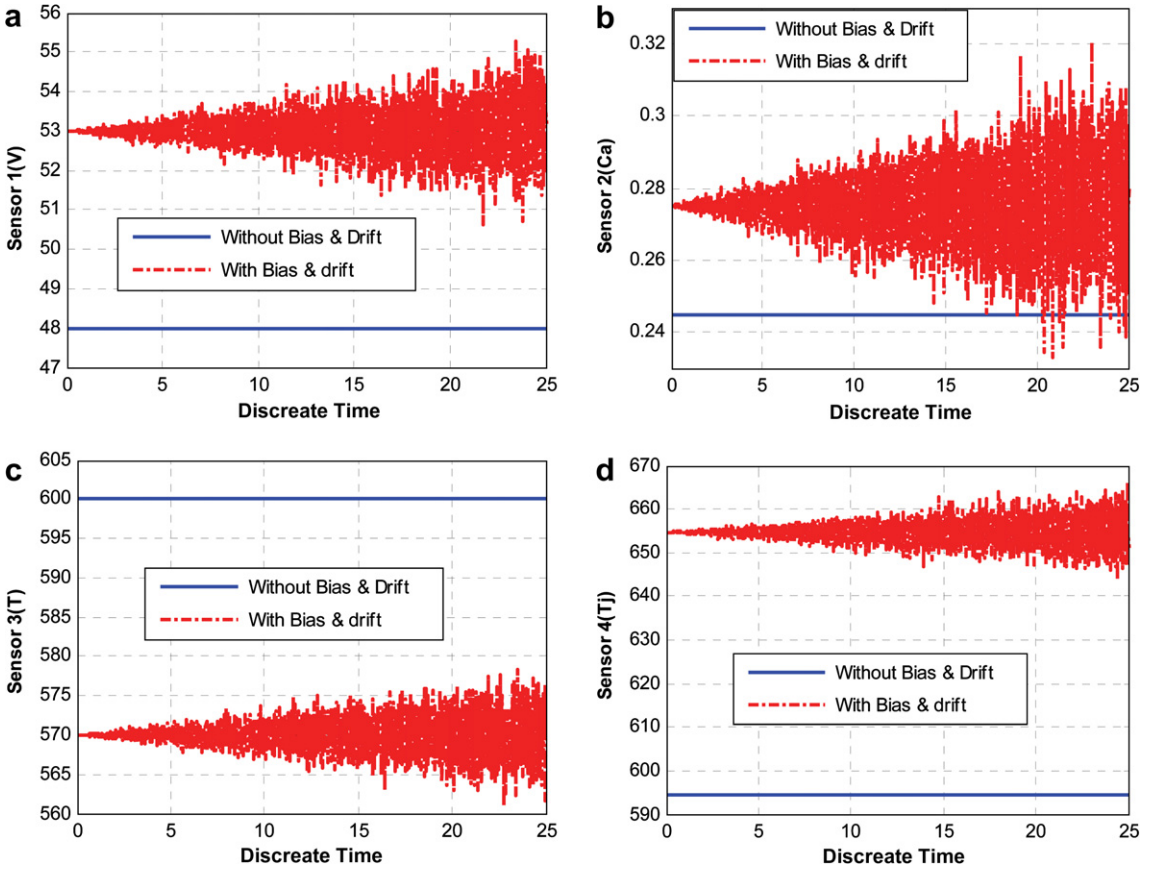

Fig. 5. Sensor faults including bias and drift, (a) sensor V, (b) sensor Ca, (c) sensor T, (d) sensor T_c.

time samples, and $N_n(k)$ is a zero-mean white Gaussian noise with unit variance and uncorrelated with process and measurement noises.

4.3.3. Simulation and results

To illustrate the application of the fault detection and identification procedures, a simulation study will be conducted in this subsection. Consider the CSTR plant described in Section 4.1. A sensor fault scenario is simulated in which the four CSTR key measured variables (V, T, Ca, T_j) are corrupted with the combined drift in their corresponding sensor calibration (bias) and degradation (excessive-variance) as summarized in Table 2.

The distributed state-vector fusion integration method is used to detect and diagnosis the sensor calibration and degradation faults. This is mainly due to the distributed nature of this method in which the filtering process is done by parallel Kalman filters, located locally at the individual sensor positions. This makes it possible to detect and isolate the sensor faults in order to differentiate the real sensor data before integrating it at the fusion center.

In this approach, the sensor bias faults are estimated by the individual EKF estimation algorithms using the augmented state variable vector including the bias vector term. While, the sensor faults due to drift in sensors degradation are detected via the residual errors ($z - H^*\hat{x}$) of each individual EKF estimates.

Fig. 5 illustrates the corrupted sensor measurements V, T, Ca, T_j due to the simultaneous occurrence of both introduced sensor faults (described in Table 2) including with the sensor data measurements due to actual fault-free for comparison purposes.

Figs. 6 and 7 demonstrate the resulting sensor fault detection and isolation in which both type of sensor faults been estimated. As shown, the faults due to the sensor biases have accurately been estimated in Fig. 6. Fig. 7 depicts the estimated sensor faults due to drift in the degradation.

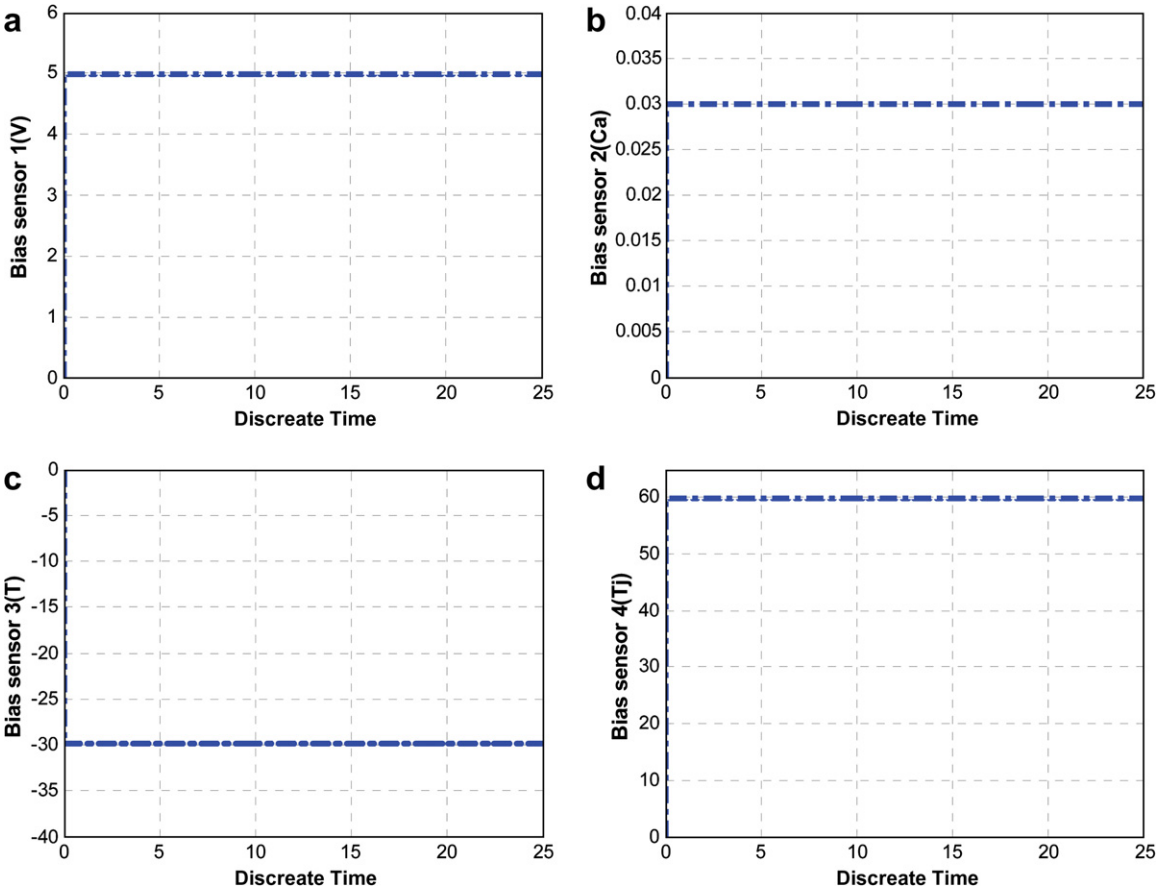

Fig. 6. Bias detection.

Please cite this article in press as: M. Mosallaei et al., Centralized and decentralized process and sensor ..., Measurement (2008), doi:10.1016/j.measurement.2008.02.009

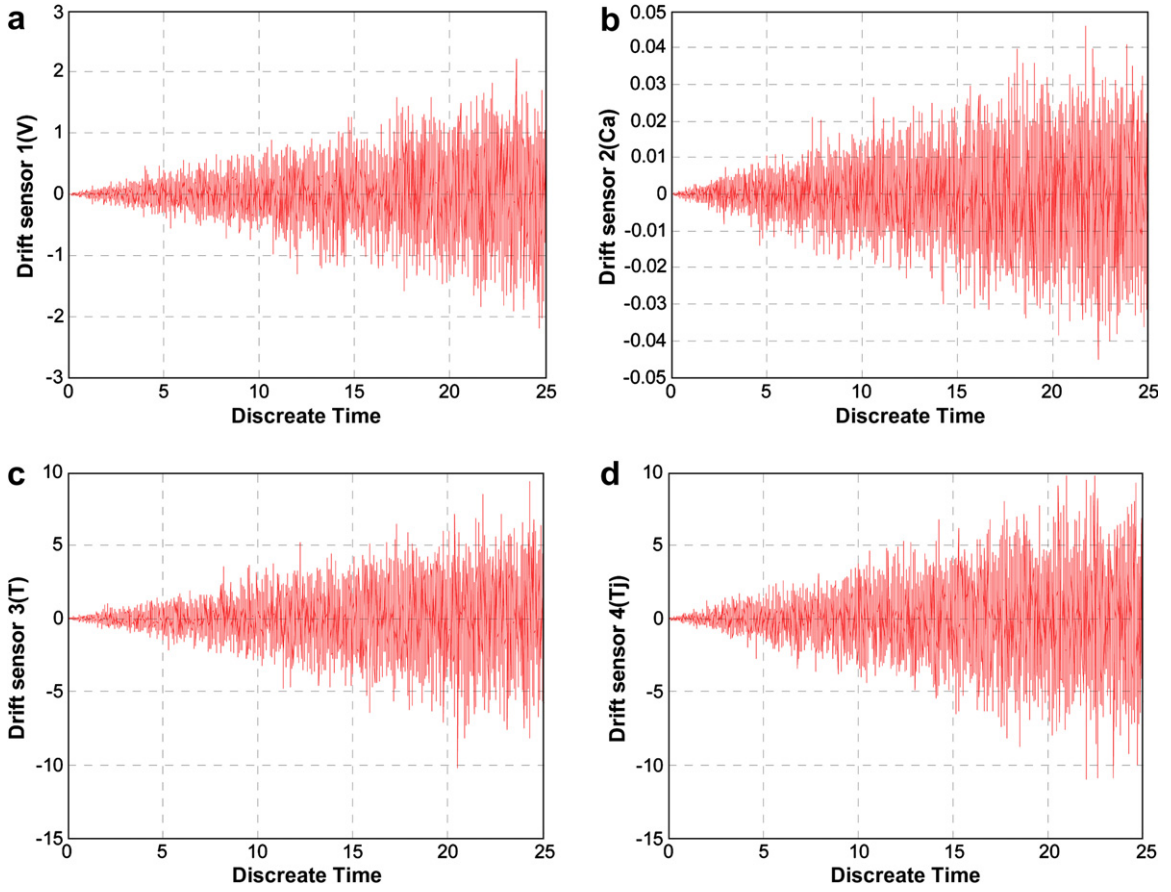

Fig. 7. Drift detection.

Table 3 summarizes the resulting drift detection accuracies calculated individually for each measured variable in terms of the root mean-squared error (RMSE) in the estimates (i.e., the difference between estimated and true values).

The obtained results indicate the superior efficiency of the proposed algorithm to detect and diagnose both types of the sensor faults. To investigate the capability of the presented algorithm to reveal the excessive-variance sensor fault, its performance is evaluated and compared with that of the independent component analysis (ICA), as an emerging powerful statistical signal processing technique, which is able to extract the hidden or underlying sensor fault noise from the measured data using the FastICA algorithm [16]. The obtained results are depicted in Figs. 8–11 for the different key measured variables.

A comparison of the RMSE measures for the both approaches, indicate that the presented algorithm in this work is able to provide more accurate estimates with respect to the ICA method.

4.4. Process fault detection and diagnosis

4.4.1. CSTR process faults

Table 4 lists some of the probable CSTR process faults.

4.4.2. Simulation and results

A series of simulation runs will be conducted on the CSTR plant to evaluate and compare the effectiveness of the two multi-sensor distributed and centralized integration approaches based on the

Table 3
Comparison of RMSE drift fault between proposed method and ICA method

Measurement variable	RMSE for the proposed method (%)	RMSE for the ICA method (%)
V	3.5466	3.4415
C_a	0.4462	0.6664
T	3.7973	17.511
T_j	3.6446	14.1558

Please cite this article in press as: M. Mosallaei et al., Centralized and decentralized process and sensor ..., Measurement (2008), doi:10.1016/j.measurement.2008.02.009

Kalman filter data fusion algorithm. To carry out the different simulation test runs under the same process fault, a predefined multi-fault test scenario is programmed. First, the inlet reactant feed is changed by a negative step of $\Delta F_i = 10\%$ at sampling instant (t) of 5. Then, the inlet reactant concentration undergoes a step change of $\Delta Ca_i = 10\%$ at $t = 10$. Following that, the inlet temperature of the reactant undergoes a negative step change of $\Delta T_i = 10\%$ at $t = 15$ and subsequently the inlet tem-

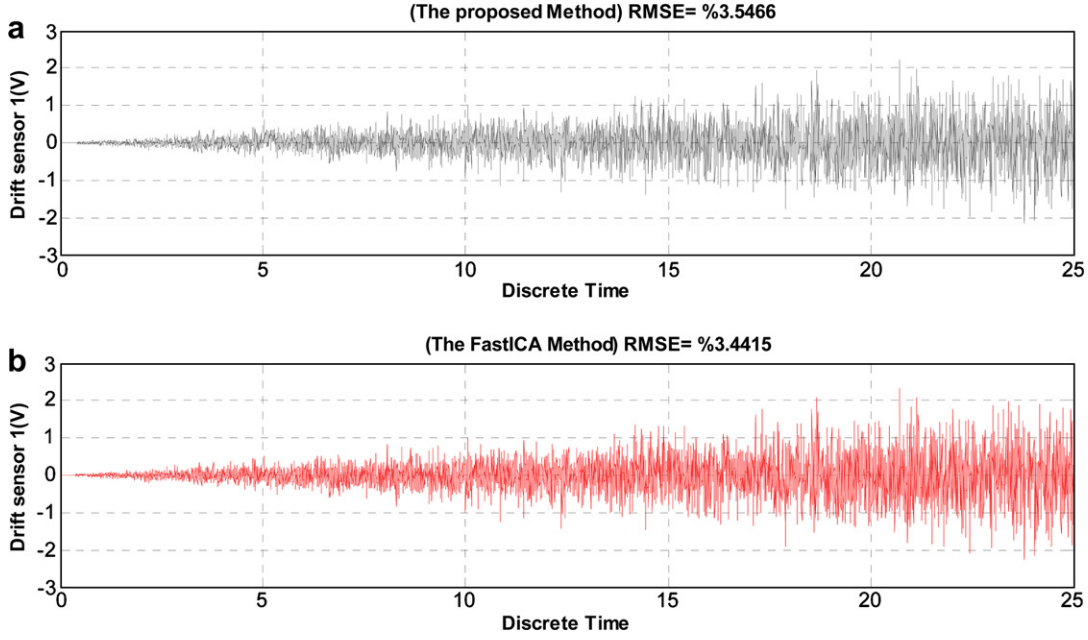

Fig. 8. Drift detection in the sensor (V). (a) The proposed method. (b) The ICA method.

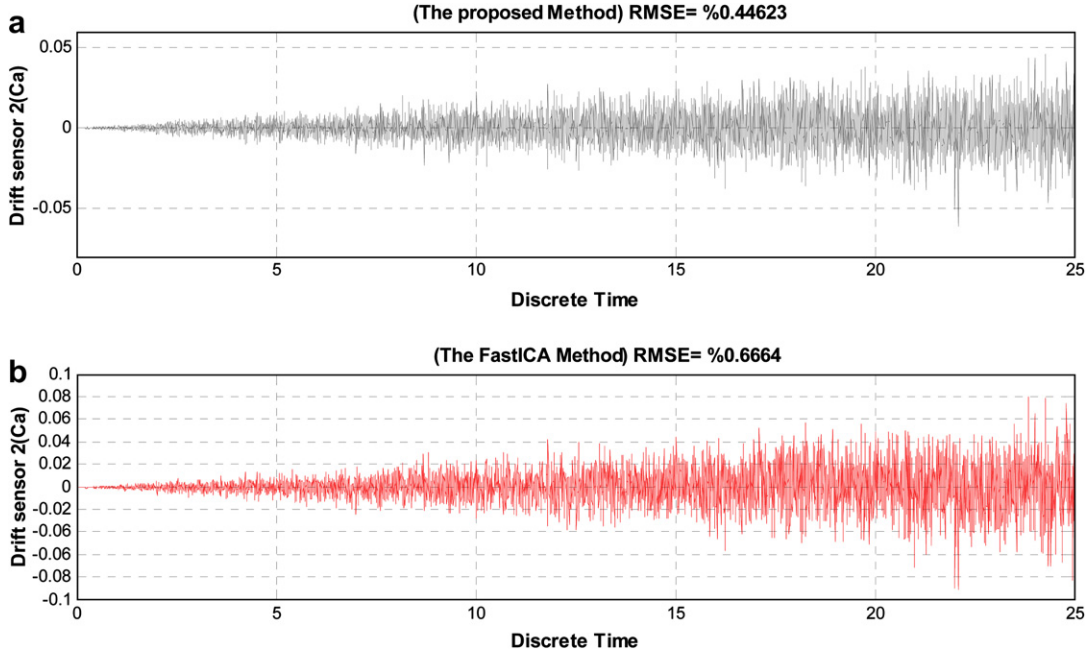

Fig. 9. Drift detection in the sensor (Ca). (a) The proposed method. (b) The ICA method.

Please cite this article in press as: M. Mosallaei et al., Centralized and decentralized process and sensor ..., Measurement (2008), doi:10.1016/j.measurement.2008.02.009

perature of coolant goes up by a step change of $\Delta T_c = 5\%$ at $t = 20$. Thus, this fault test scenario embodies a complete simulation picture in which single, double, triple and finally quadruple process faults occur sequentially after a 5 sampling time interval.

Three different simulation runs, corresponding to three different process monitoring approaches, i.e., non-adaptive centralized output augmented fusion (OAF) or (NACOAF) method, adaptive centralized OAF (ACOAF) method and adaptive distributed state-vector fusion (ADSVF) method, were carried

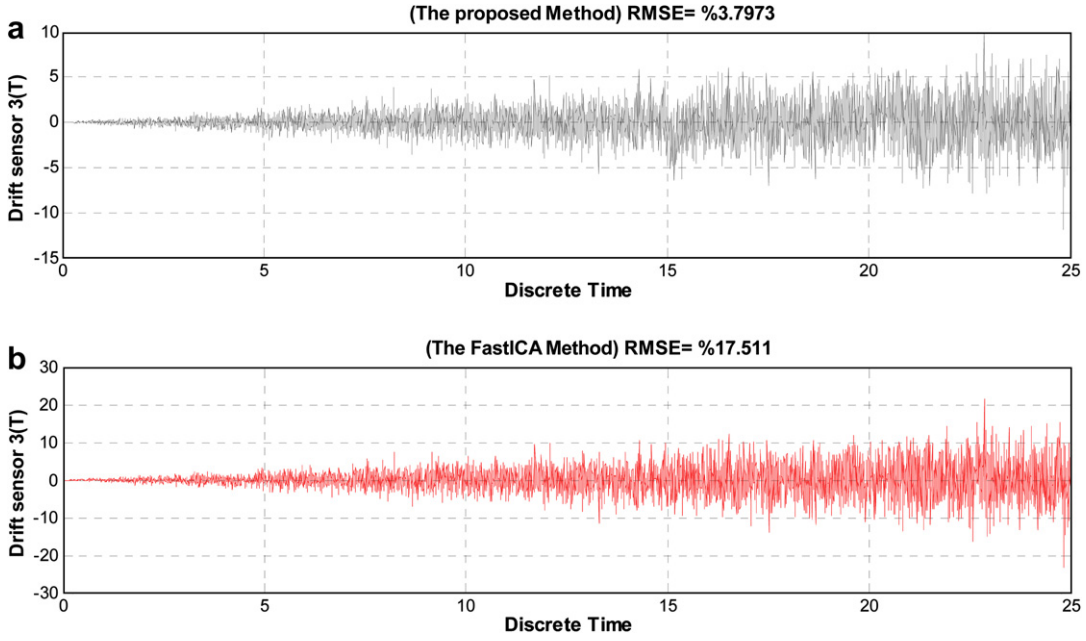

Fig. 10. Drift detection in the sensor (T). (a) The proposed method. (b) The ICA method.

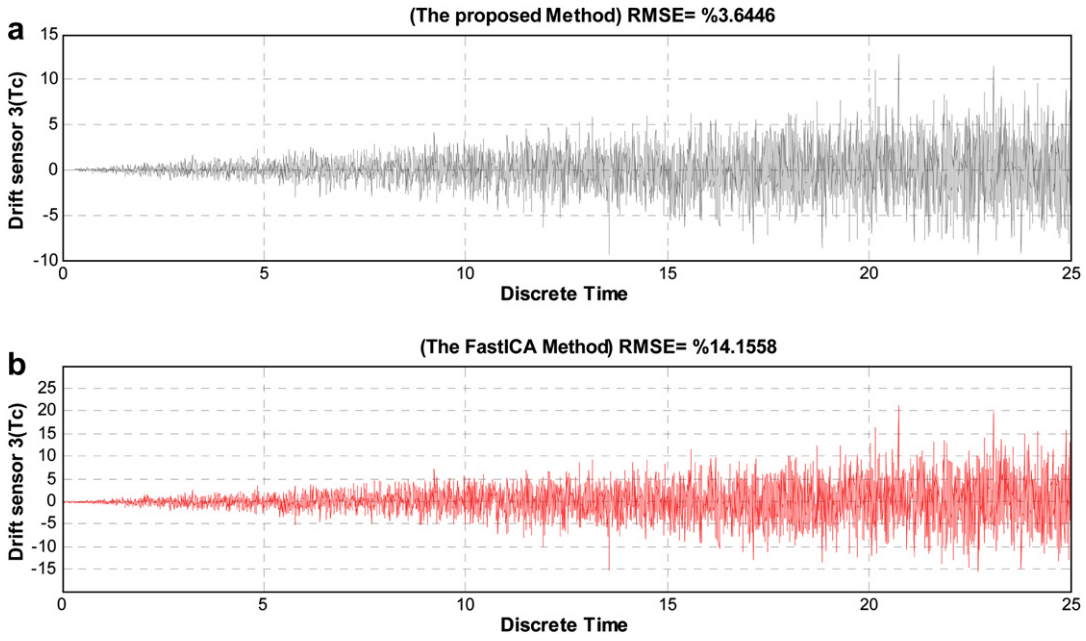

Fig. 11. Drift detection in the sensor (T_c). (a) The proposed method. (b) The ICA method.

Please cite this article in press as: M. Mosallaei et al., Centralized and decentralized process and sensor ..., Measurement (2008), doi:10.1016/j.measurement.2008.02.009

Table 4
List of process faults

Fault number	Fault name	Notation
1	Low inlet feed of reactant	dF_i
2	High inlet concentration of reactant	dCa_i
3	Low inlet temperature of reactant	dT_i
4	High inlet temperature of coolant	dT_c

out. Fig. 12 demonstrates the resulting process fault estimation outcomes due to the foregoing three monitoring approaches.

In order to clarify the assessment of the monitoring performances, the corresponding errors in the resulting fault estimation are depicted in Fig. 13.

Noting that all the fault monitoring approaches have been evaluated on the same measured data for the same realizations of the fault test scenario. The resulting observations demonstrate that the ACOAF method generally present better fault estimation performance in terms of the resulting RMSE measures, summarized in Table 5.

However, ADSVF method has a lower computation time and communication cost and benefits the advantage of parallel distributed implementation, leading to a higher fault-tolerant capability.

5. Conclusions

This paper addresses the sensor and process fault monitoring problem using multi-sensor data fusion technique based on EKF estimation algorithm. A discrete-time EKF approach has been adapted to enhance the robustness of its implementation. The process and sensor bias faults have been treated as extra states from the monitoring perspective, leading to a new augmented state-space model formulation. A new adaptive EKF algorithm has been developed to include the time-varying nature of process and measurement noises in the estimation algorithm. To realize this uncertainty adaptation, the innovation and residual errors information have been incorporated in the developed online relationships, to update the process and measurement covariance matrices. This adaptive scheme increases the accuracy of the estimation and prevents the

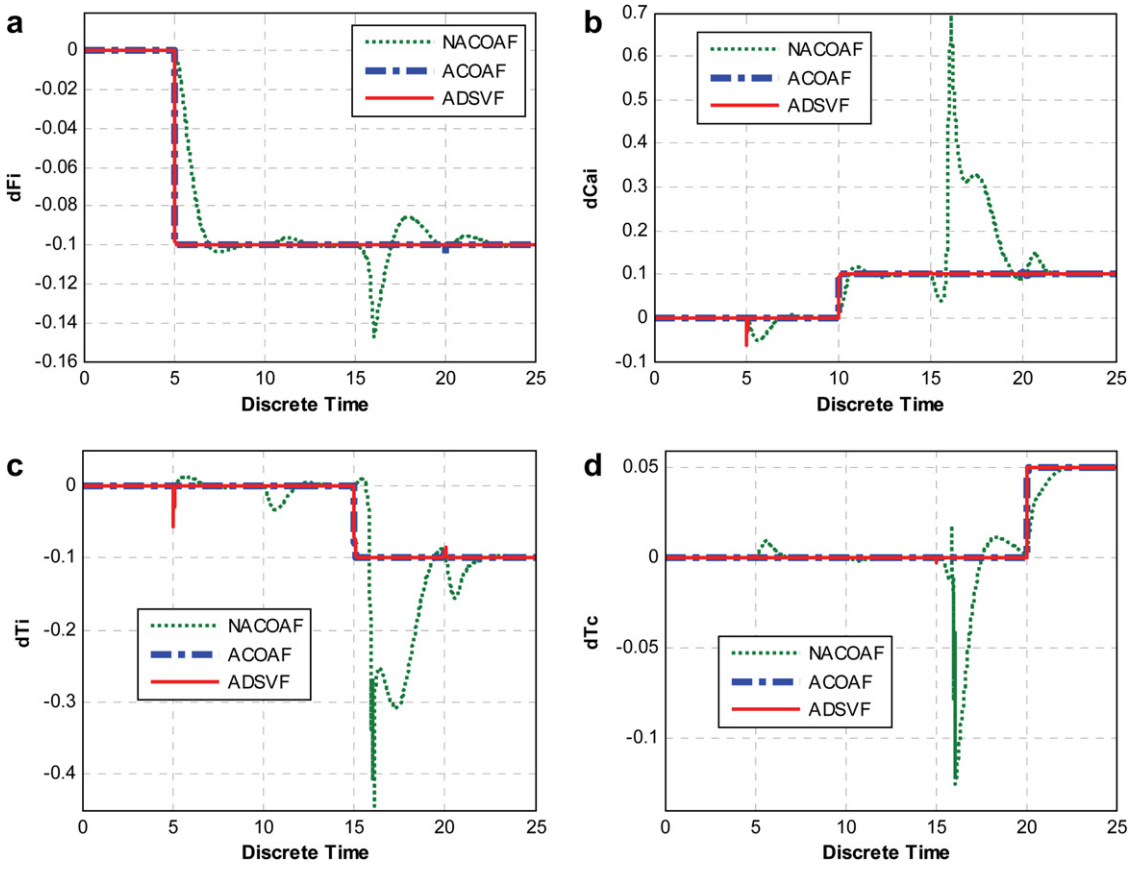

Fig. 12. Estimation of faults occurring at different times with different magnitudes.

Please cite this article in press as: M. Mosallaei et al., Centralized and decentralized process and sensor ..., Measurement (2008), doi:10.1016/j.measurement.2008.02.009

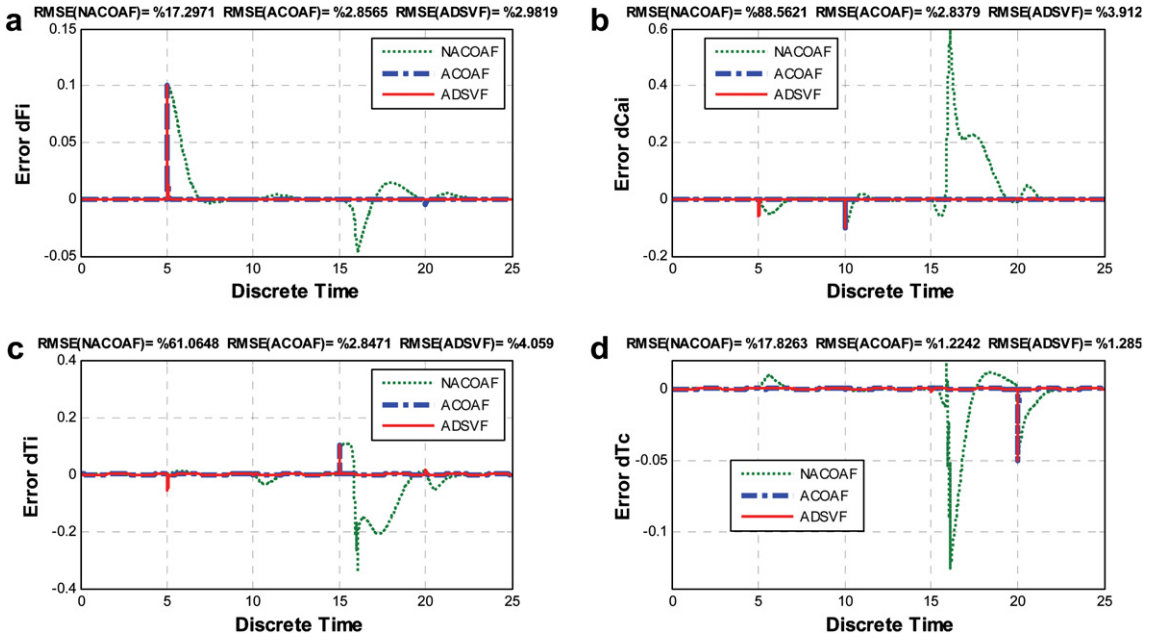

Fig. 13. The fault estimation errors and their RMSE.

Table 5
Resulting RMSE measures and computation time

Method	RMSE of process faults (%)				Computation time (s)
	dF_i	dCa_i	dT_i	dT_c	
NACOAF	17.2971	88.5621	61.0648	17.8263	15.6941
ACOAF	2.8565	2.8379	2.8471	1.2242	26.7952
ADSVF	2.9819	3.9120	4.0590	1.2850	15.3771

EKF algorithm to degrade its performance. Two different centralized and distributed multi-sensor integration architectures were presented based on the non-adaptive and adaptive EKF data fusion algorithms to monitor sensor and process faults.

A set of simulation studies were conducted on a CSTR benchmark problem to investigate the performances of the proposed monitoring methods. The sensor fault study focused on drift in sensor calibration (i.e., bias error) and drift in sensor degradation (i.e., excessive-variance noise) anomalies. The process fault study included four probable CSTR process faults listed in Table 4.

The sensor bias faults were estimated accurately using the individual EKF algorithms based on the augmented state variable vector including the bias vector terms. While, sensor faults due to drifts were estimated via the EKF residual estimation errors. Comparison of the resulting sensor drift fault monitoring to that of the ICA method, as a powerful noise separation approach, revealed a better performance in terms of the obtained RMSE measure.

Three different proposed monitoring approaches, i.e. NACOAF, ACOAF and ADSVF, were tested on the CSTR plant to evaluate their performance against process faults using a series of simulation studies. The resulting performances, summarized in Table 5, demonstrate that the ACOAF method can generally present a better fault estimation from the RMSE measure point of view. However, ADSVF method has the advantages of parallel distributed architecture, benefiting a lower computation time and communication cost and higher fault-tolerant characteristic.

References

[1] W.S. Lee, D.I. Grosh, F.A. Tillman, C.H. Lie, Fault tree analysis, methods and applications: a review, IEEE Trans. Reliab. R-34 (1985) 194–302.

Please cite this article in press as: M. Mosallaei et al., Centralized and decentralized process and sensor ..., Measurement (2008), doi:10.1016/j.measurement.2008.02.009

[2] M.A. Kramer, B.L. Palowitch Jr., A rule based approach to fault diagnosis using the signed directed graph, AIChE J. 33 (7) (1987) 1067–1078.
[3] W.L. Cao, B.S. Wang, L.Y. Ma, J. Zhang, J.Q. Gao, Fault diagnosis approach based on the integration of qualitative model and quantitative knowledge of signed directed graph, in: Proceedings of the Fourth International Conference on Machine Learning and Cybernetics, Guangzhou, 2005, pp. 2251–2256.
[4] P. Vaija, I. Turunen, M. Jarvelainen, M. Dohnal, Fuzzy strategy for failure detection and safety control of complex processes, Microelectr. Reliab. 25 (2) (1985) 369–381.
[5] R. Fickelsherer, D.E. Lamb, P. Dhujati, D.L. Chester, Role of dynamic simulation in developing an expert system for chemical process fault detection, in: Proceedings of the Computer Simulation Conference Society for Computer Simulation, 1986.
[6] Yih-Yuan Hsu, Cheng-Ching Yu, A self-learning fault diagnosis system based on reinforcement learning, Am. Chem. Soc. 31 (1992) 1937–1946.
[7] R. Isermann, Process fault detection based on modeling and estimation methods, a survey, Automatica (1984) 387–404.
[8] D.M. Himmelblau, Fault Detection and Diagnosis in Chemical and Petrochemical Processes, Elsevier, Amsterdam, 1978.
[9] A.S. Willsky, A survey of design methods for failure detection systems, Automatica (1976) 601–611.
[10] P.S. Maybeck, Stochastic Models, Estimation and Control, vols. I and II, Academic Press, New York, 1982.
[11] Q. Gan, C.J. Harris, Comparison of two measurement fusion methods for Kalman-filter-based multi-sensor data fusion, IEEE Trans. Aerospace Electr. System 37 (1) (2001) 273–280.
[12] C. Harris, X. Hong, Q. Gan, Adaptive Modeling, Estimation and Fusion from Data: A Neurofuzzy Approach, Springer, 2001.
[13] M.S. Schlosser, K. Kroschel, Communication issues in decentralized Kalman filters, Fusion (2004), IF04-0731.
[14] W.L. Luyben, Process Modeling Simulation and Control for Chemical Engineers, second ed., McGraw-Hill, 1989.
[15] N. Sawattanakit, V. Jaovisidha, Process fault detection and diagnosis in CSTR system using on-line approximator, IEEE (1998) 747–750.
[16] A. Hyvarines, E. Aja, A fast fixed-point algorithm for independent component analysis, Neural Comput. 9 (1997) 1483.

Please cite this article in press as: M. Mosallaei et al., Centralized and decentralized process and sensor ..., Measurement (2008), doi:10.1016/j.measurement.2008.02.009